*Under One Sky: The IAU Centenary Symposium*
*Proceedings IAU Symposium No. ,*
doi:

# Milliarcsecond Core Size Dependence of the Radio Variability of Blazars

**Po-Chih Hsu,[1,2] Jun Yi Koay,[1] Satoki Matsushita,[1] Chorng-Yuan Hwang,[2] Talvikki Hovatta,[3,4] Sebastian Kiehlmann,[5,6,7] Walter Max-Moerbeck,[8] Tim Pearson,[5] Anthony Readhead,[5] Rodrigo Reeves,[9] Harish Vedantham[10,11]**

[1]Institute of Astronomy and Astrophysics, Academia Sinica, Taipei 10617, Taiwan (R.O.C.)
[2]Graduate Institute of Astronomy, National Central University, Taoyuan 32001, Taiwan (R.O.C.)
[3]Finnish Centre for Astronomy with ESO (FINCA), University of Turku, FI-20014 Turku, Finland
[4]Aalto University Metsähovi Radio Observatory, Metsähovintie 114, FI-02540 Kylmälä, Finland
[5]Owens Valley Radio Observatory, California Institute of Technology, Pasadena, CA 91125, USA
[6]Institute of Astrophysics, Foundation for Research and Technology-Hellas, GR-71110 Heraklion, Greece
[7]Department of Physics, University of Crete, GR-70013 Heraklion, Greece
[8]Departamento de Astronomía, Universidad de Chile, Camino El Observatorio 1515, Las Condes, Santiago, Chile
[9] Departamento de Astronomía, Universidad de Conceptión, Concepción, Chile
[10]Cahill Center for Astronomy and Astrophysics, California Institute of Technology, 1200 E. California Blvd., Pasadena, CA 91125, USA
[11]Netherlands Institute for Radio Astronomy (ASTRON), Oude Hogeveensedijk 4, NL-7991 PD Dwingeloo, the Netherlands

**Abstract.** Studying blazar radio variability on timescales ranging from months to years provides information on the sub-parsec-scale structures of the jets, and the physics of the central active galactic nuclei. In this study, we focus on the radio variability of 1158 blazars observed at 15 GHz through the Owens Valley Radio Observatory Blazar Monitoring Program, where these sources have been observed about twice a week for over a decade. We investigate the dependence of the variability amplitudes and timescales, derived using a simple model fit to the structure function, on the milliarcsecond radio core sizes measured by Very Long Baseline Interferometry. The most compact sources exhibit larger variability amplitudes and shorter variability timescales than the more extended sources; this could be explained by light travel-time effects.

**Keywords.** galaxies: active – galaxies: jets – quasars: general

## 1. Introduction

Radio variability of active galactic nuclei (AGNs) provides an opportunity to study the physics of the most compact regions of super massive black holes. Blazar variability can originate from the shocks produced along the jet (Hughes et al. 1985, Hovatta et al. 2008), jet precession (Kudryavtseva et al. 2011), variable accretion rates due to disk instabilities (Lin & Shields 1986), or tidal disruption events (Alexander et al. 2020), among others causes. Blazars, a subclass of AGN with relativistic jets aligned at a small angle to our line of sight, are suitable for such studies due to their compact and variable nature.

In this study, we used radio variability data from the 15 GHz Owens Valley Radio Observatory (OVRO) blazar monitoring program (Richards et al., 2011), where more than 1500 blazars have been observed for over a decade, providing a large blazar sample with good time sampling (typical cadence of about 4 days). We used 1158 sources selected from the Candidate Gamma-Ray Blazar Survey (CGBaBS, Healey et al. 2008). We also make use of multi-frequency blazar core sizes (1-86 GHz) derived by Koryukova et al. (2022), which extends the work of an earlier paper by Pushkarev & Kovalev (2015). The core sizes were

derived by fitting two circular Gaussian component models (Kovalev et al. 2005) to the self-calibrated VLBA visibilities for each of their sources, with the most compact component being considered to be the core component.

We cross match the OVRO sample with the Koryukova et al. (2022) sample with core size measurements. There are 116, 865, 464, 1053, 376, 156, 158, and 1 OVRO source(s) with available core size measurements at 1, 2, 5, 8, 15, 24, 43, and 86 GHz, respectively. In this study, we used angular core sizes from 2 to 43 GHz to investigate the dependency of variability amplitudes and timescales on the core sizes.

## 2. Analysis

We used the structure function (SF) to characterize the variability of the sources. The observed structure function $D_{\rm obs}(\tau)$ at a given time lag $\tau$ is given by:

$$D_{\rm obs}(\tau) = \frac{1}{N_\tau}\sum_{j,k}[S(t_{\rm j}) - S(t_{\rm k} - \tau)]^2 \tag{1}$$

where $S(t)$ is the measured flux density at time $t$, normalized by the mean flux density, and $N_\tau$ is the number of pairs of flux densities with a time lag $\tau$. Next, we fit a simple model to the SF, assuming the variations are stochastic in nature, given by,

$$D_{\rm mod}(\tau) = D(1000{\rm d})\frac{1+\tau_{\rm char}/1000}{1+\tau_{\rm char}/\tau} + {\rm D}_{\rm noise} \tag{2}$$

where $D(1000{\rm d})$ is the SF amplitude at 1000 days, $\tau_{\rm char}$ is the characteristic variability timescale, and $D_{\rm noise}$ is a constant additive noise floor due to systematic and instrumental errors that contribute to the overall variability.

For our analysis, we use the SF amplitude at 1000 days, derived from the above model fit, to characterize the long term variability amplitudes. We define the characteristic timescale of variability, as the time lag at which the SF amplitude reaches half the maximum of the saturation value.

## 3. Results and Discussion

### 3.1. *Dependence of Variability Amplitude on Core Sizes*

To test the dependence of variability amplitudes at 1000 days with angular core sizes, we separate the sources into strong ($\theta_{\rm strong}$) and weak variables ($\theta_{\rm weak}$), based on the median value of the variability amplitudes at 1000 days ($\tilde{D}(1000{\rm d})$). We then compare the distributions of the angular core sizes of the strong (blue histograms) and weak (orange histograms) variables, as shown in figure 1. We performed the two sample K-S test (results presented in table 1 test A), and found that weak variable sources (orange histograms) have significantly larger angular core sizes than strong variable (blue histograms) sources. The p-value is larger at 15 GHz compared to that at 8 GHz, likely due to the smaller sample size.

### 3.2. *Dependence of Variability Timescale on Core Sizes*

For each frequency at which the core size measurements are available, we separate the source sample into fast ($\theta_{\rm fast}$) and slow variables ($\theta_{\rm slow}$), based on the median of the characteristic timescale ($\tilde{\tau}_{\rm char}$). Figure 2 displays the distribution of the angular sizes of the fast (orange histograms) and slow (blue histograms) variables. We also perform two sample K-S tests comparing the distributions. We found that for core sizes measured at 2, 8, 15, and 24 GHz, the fast variable sources have significantly smaller angular core sizes than slow variable sources (see table 1 test B).

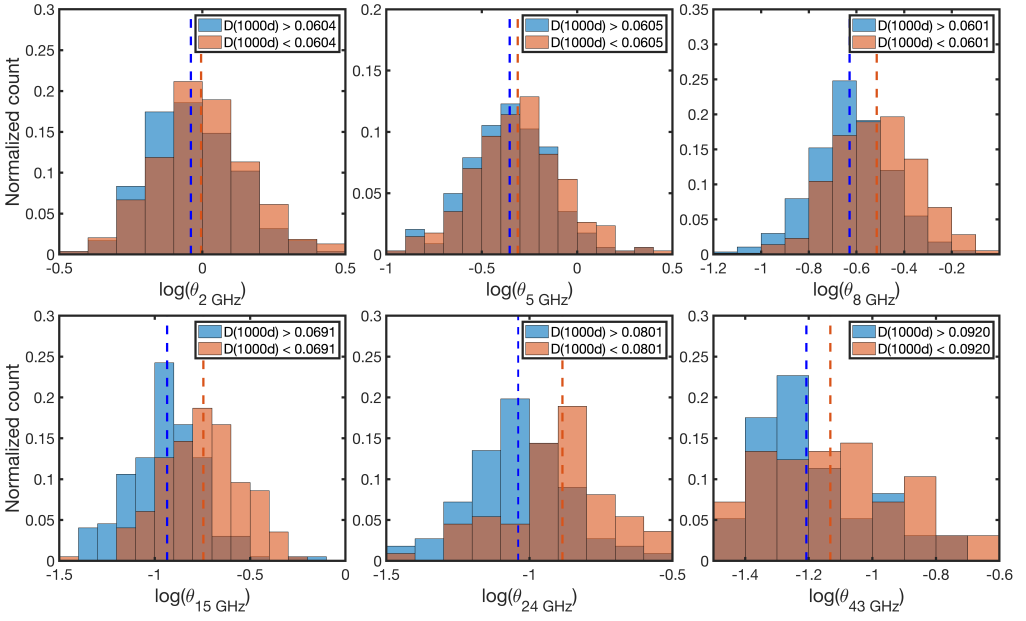


**Figure 1.** Normalized distributions of angular core sizes ($\theta$) at different frequencies, separated into strong and weak variables by the median of the 15 GHz variability amplitudes $D$(1000d). The blue and orange dashed lines show the median value of the angular core sizes of the strong and weak variables, respectively. The brown areas correspond to overlapping regions between the blue and orange histograms.

**Table 1.** Results of two sample K-S test. Test A is the K-S test comparing the distribution of angular core sizes of weak and strong variables at 6 frequencies; test B is the K-S test comparing the distribution of angular core sizes of slow and fast variables at 6 frequencies. Sample sizes, median variability amplitudes at 1000 days $\tilde{D}$(1000d) or median of characteristic timescale $\tilde{\tau}_{\rm char}$, median core sizes of each distribution, as well as $p$ value of each test are given in the table.

| Test A (Separated by $\tilde{D}$(1000d)) | Sample number | $\tilde{D}$(1000d) | $\tilde{\theta}_{\rm weak}$ [mas] | $\tilde{\theta}_{\rm strong}$ [mas] | p value |
|---|---|---|---|---|---|
| Distribution of $\theta_{2\ \rm GHz,weak}$ and $\theta_{2\ \rm GHz,strong}$ | 865 | 0.0604 | 0.99 | 0.91 | $1.83 \times 10^{-2}$ |
| Distribution of $\theta_{5\ \rm GHz,weak}$ and $\theta_{5\ \rm GHz,strong}$ | 464 | 0.0605 | 0.49 | 0.45 | $1.30 \times 10^{-1}$ |
| Distribution of $\theta_{8\ \rm GHz,weak}$ and $\theta_{8\ \rm GHz,strong}$ | 1053 | 0.0601 | 0.31 | 0.24 | $7.77 \times 10^{-17}$ |
| Distribution of $\theta_{15\ \rm GHz,weak}$ and $\theta_{15\ \rm GHz,strong}$ | 376 | 0.0691 | 0.18 | 0.12 | $2.58 \times 10^{-15}$ |
| Distribution of $\theta_{24\ \rm GHz,weak}$ and $\theta_{24\ \rm GHz,strong}$ | 156 | 0.0801 | 0.13 | 0.09 | $1.58 \times 10^{-6}$ |
| Distribution of $\theta_{43\ \rm GHz,weak}$ and $\theta_{43\ \rm GHz,strong}$ | 158 | 0.0920 | 0.07 | 0.06 | $5.78 \times 10^{-2}$ |
| **Test B (Separated by $\tilde{\tau}_{\rm char}$)** | **Sample number** | **$\tilde{\tau}_{\rm char}$ [days]** | **$\tilde{\theta}_{\rm slow}$ [mas]** | **$\tilde{\theta}_{\rm fast}$ [mas]** | **p value** |
| Distribution of $\theta_{2\ \rm GHz,slow}$ and $\theta_{2\ \rm GHz,fast}$ | 965 | 650 d | 0.99 | 0.91 | $4.72 \times 10^{-4}$ |
| Distribution of $\theta_{5\ \rm GHz,slow}$ and $\theta_{5\ \rm GHz,fast}$ | 464 | 637 d | 0.50 | 0.44 | $1.78 \times 10^{-1}$ |
| Distribution of $\theta_{8\ \rm GHz,slow}$ and $\theta_{8\ \rm GHz,fast}$ | 1053 | 630 d | 0.25 | 0.28 | $1.07 \times 10^{-4}$ |
| Distribution of $\theta_{15\ \rm GHz,slow}$ and $\theta_{15\ \rm GHz,fast}$ | 376 | 560 d | 0.16 | 0.12 | $2.33 \times 10^{-6}$ |
| Distribution of $\theta_{24\ \rm GHz,slow}$ and $\theta_{24\ \rm GHz,fast}$ | 156 | 544 d | 0.12 | 0.10 | $4.52 \times 10^{-2}$ |
| Distribution of $\theta_{43\ \rm GHz,slow}$ and $\theta_{43\ \rm GHz,fast}$ | 158 | 482 d | 0.07 | 0.06 | $6.33 \times 10^{-2}$ |

## 4. Discussion and Conclusion

We found significant differences in the distribution of the angular core sizes of the strong and weak variables. This is true of angular core sizes not only that measured at 15 GHz where the variability is observed, but also at other frequencies (i.e., 2-24 GHz). This can

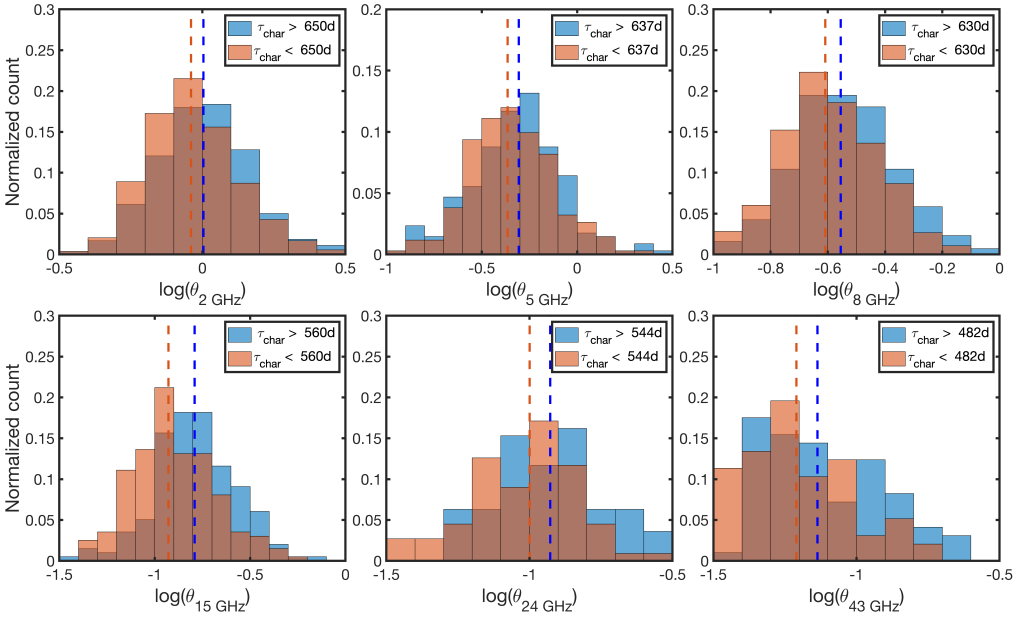


**Figure 2.** Normalized distributions of angular core size ($\theta$) of slow and fast variables, separated by the median of characteristic timescales $\tau_{\rm char}$. The blue and orange dashed lines show the median of angular core sizes of the slow and fast variables at each frequency. The brown areas correspond to overlapping regions between the blue and orange histograms.

be explained if the jets have a frequency-core size relationship, e.g., following the conical jet model (Ghisellini & Tavecchio (2009)). The fact that we found that fast variable sources have significantly smaller angular core sizes, compared to the slow variable sources, can be explained by the light travel time argument. We are investigating the relationship between variability amplitudes/timescales with linear core sizes, for sources with redshift information (Hsu et al., in prep).

## Acknowledgements

This research has made use of data from the OVRO 40-m monitoring program (Richards, J. L. et al. 2011, ApJS, 194, 29), supported by private funding from the California Institute of Technology and the Max Planck Institute for Radio Astronomy, and by NASA grants NNX08AW31G, NNX11A043G, and NNX14AQ89G and NSF grants AST-0808050 and AST-1109911.

## References

Alexander K. D. et al., 2020, *Space Sci. Rev.*, 216, 81
Ghisellini G. and Tavecchio F., 2009, *MNRAS*, 397, 985
Healey S. E. et al., 2008, *ApJS*, 175, 97
Hovatta T. et al., 2008, *A&A*, 485, 51
Hughes P. A., Aller H. D. and Aller M. F., 1985, *ApJ*, 298, 301
Koryukova T. A. et al., 2022, *MNRAS*, 515, 1736
Kovalev Y. Y. et al., 2005, *AJ*, 130, 2473
Kudryavtseva N. A. et al., 2011, *A&A*, 526, A51
Lin D. N. C. and Shields G. A., 1986, *ApJ*, 305, 28

Pushkarev A. B. and Kovalev Y. Y., 2015, *MNRAS*, 452, 4274
Richards J. L. et al., 2011, *ApJS*, 194, 29